Performance Characterization of Visible Light Communication Based on GaN High-Voltage LED/PD

LU Meixin, JIANG Zitong, FANG Li, YAN Yiqun, YAN Jiabin

(Nanjing University of Posts and Telecommunications, Nanjing 210003, China)

Abstract: While considerable research has been conducted on the structural principles, fabrication techniques, and photoelectric properties of high-voltage light-emitting diodes (LEDs), their performance in light communication remains underexplored. A high-voltage series-connected LED or photodetector (HVS-LED/PD) based on the gallium nitride (GaN) integrated photoelectronic chip is presented in this paper. Multi-quantum wells (MQW) diodes with identical structures are integrated onto a single chip through wafer-scale micro-fabrication techniques and connected in series to construct the HVS-LED/PD. The advantages of the HVS-LED/PD in communication are explored by testing its performance as both a light transmitter and a PD. The series connection enhances the device's 3 dB bandwidth, allowing it to increase from 1.56 MHz to a minimum of 2.16 MHz when functioning as an LED, and from 47.42 kHz to at least 85.83 kHz when operating as a PD. The results demonstrate that the light communication performance of HVS-LED/PD is better than that of a single GaN MQW diode with bandwidth and transmission quantity, which enriches the research of GaN-based high-voltage devices.

Keywords: high-voltage LEDs; high-voltage PDs; GaN MQW diode array; communication characterization; visible light communication

1 Introduction

Light-emitting diodes (LEDs) are solid-state semiconductor devices that can convert electrical signals into visible light signals, featuring high energy efficiency, low power, and fast response speed[1−3]. With the development of semiconductor technology, LED has been widely used in electronic screen displays, home/street lighting, and other fields, in which high-power LEDs have garnered significant attention[4−6]. High-power LED devices have important application potential in visible light communication (VLC)[7−9], especially long-distance communications. Enlarging the device size is a common method for realizing a high-power LED[10−11]. However, large LEDs easily suffer from uneven current distribution and efficiency drop[12−13]. Another type of high-power LED is obtained by connecting several small-sized LEDs in series[14−15], called high-voltage series-connected (HVS) LED. The HVS-LED exhibits a low operating current and effectively addresses the issue of overcrowded current, leading to reduced alternating current/direct current (AC/DC) conversion power loss, enhanced reliability, and lower packaging cost[16−18].

Previously published works on HVS-LED mainly focus on optical characterization[19−20] and fabrication technologies[21−22]. However, only a few reports studied the influence of series structure on the light communication performance of the HVS-LED. Moreover, the performance of gallium nitride (GaN) multi-quantum wells (MQW) photodiodes (PDs) in series also has not been explored. Recently, advancements in the communication performance of LEDs and PDs have promoted their applications in high-speed data transmission and optical measurements, encompassing high-speed imaging and videography[23], time-resolved fluorescence sensing[24], motion detection[25], and numerous other fields[26−27]. Therefore, this paper proposes a visible light communication system based on GaN HVS-LED/PD and comprehensively characterizes the

system's performance with varying numbers of components connected in series.

2 Device Structure and Fabrication

The HVS-LED chip integrates 36 GaN-based MQW diodes of an identical structure. The device size is 7.6 mm × 7.6 mm and the size of each diode is 1.25 mm × 1.25 mm. A serpentine circuit configuration is employed, resulting in a more uniform current distribution across the chip. Figs. 1a and 1b reveal the chip images when one LED and five LEDs are working, respectively. Fig. 1c displays the three-dimensional structure of the chip. The comb metal is the p-electrode of the LED, which is designed to make the current distribution more uniform while shielding the light emission minimally. The ring metal is the n-electrode of the LED. Multiple LEDs are connected in series on the chip by connecting the p-electrode of the former LED and the n-electrode of the latter LED.

The epilayer structure diagram of the chip is illustrated in Fig. 1d. The GaN-based epitaxial layers on the sapphire substrate consist of an n-GaN layer, an MQW layer, and a p-GaN layer from bottom to top. The GaN chip is fabricated using a wafer-level manufacturing process. The details are described as follows. First, a transparent indium tin oxide (ITO) thin film layer is grown on the p-GaN layer by magnetron sputtering. Second, a photoresist is coated and exposed, revealing the areas to be etched, and wet etching is processed to pattern the ITO layer. Then, inductively coupled plasma (ICP) dry etching is used for the n-GaN layer. Third, the coated and exposed photoresist reveals the areas of isolation trenches, and the ICP dry etching is applied to the underlying sapphire substrate. Fourth, a photoresist layer is spin-coated on a wafer and patterned to the geometry of Metal I by lithography. Metal I is then depos-

ited by the electron beam evaporation and patterned by the lift-off process. Fifth, a layer of silicon dioxide (SiO_2) is grown on the GaN layer using plasma-enhanced chemical vapor deposition (PECVD). Subsequently, the SiO_2 layer is patterned to form the through-holes between metal layers. Sixth, a photoresist layer is coated and patterned to the geometry of Metal II by lithography. Metal II is then deposited by the electron beam evaporation and patterned by the lift-off process. Finally, the wafer is thinned and cut into separate chips of HVS-LED.

3 Photoelectric Characteristics

The current-voltage (IV) characteristics of the HVS-LED are measured using a semiconductor device analyzer (Agilent Technologies B1500A), and the results are displayed in Fig. 2a. An individual LED operates at a turn-on voltage of about 2.4 V and the turn-on voltage of the device is proportional to the number of LEDs in series, as shown in Fig. 2b. For the array with 36 LEDs in series, the turn-on voltage is about 84.6 V.

The external quantum efficiency (EQE) of the LED device is measured using an integrating sphere (Labsphere) equipped with a calibrated detector. The EQE curves for a single LED and five LEDs in series versus injection current are shown in Fig. 2c. The EQE of the five LEDs connected in series is marginally greater than that of an individual LED. The peak EQE of a single LED is 44.46% achieved at the injection current of 13 mA. As a comparison, the peak EQE of the five LEDs in series is 45.15% achieved at the injection current of 17 mA. The results indicate that the series array of LEDs can increase the output light power without introducing obvious current spreading issues that would deteriorate the efficiency of the device.

Fig. 2d demonstrates a linear rise in light output power with the injection current. Under identical current conditions, the optical power output of LEDs connected in series surpasses that achieved by a single LED configuration.

The capacitance-voltage (CV) curves for different numbers of LEDs in series are measured by the semiconductor device analyzer (Agilent Technologies B1500A) at a measurement frequency of 100 kHz, as shown in Fig. 2e. The device capacitance decreases with the increase of LED quantity in series. The reciprocal of the total capacitance of the series capacitor is equal to the sum of the reciprocal capacitance of each capacitor.

The curve on the left side of Fig. 2f presents the response spectrum (RS) of a single GaN MQW LED under zero bias voltage. The curves on the right side of Fig. 2f depict the electroluminescence
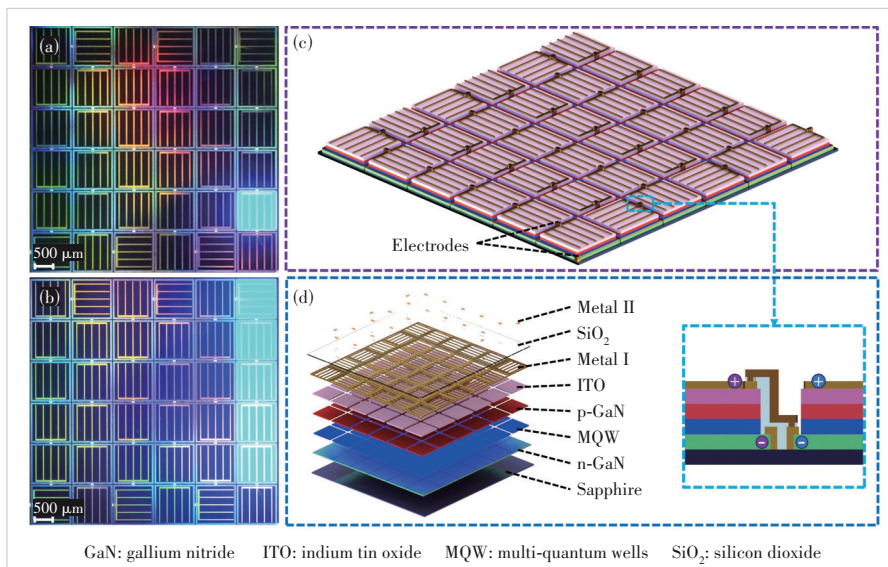
▲ Figure 1. Morphology of HVS-LED: (a) optical image of the fabricated chip with one LED illuminated; (b) optical image of the fabricated chip with five LEDs illuminated; (c) three-dimensional structure of the chip; (d) chip epilayer structure, where the inset shows the details of electrode connection

GaN: gallium nitride　　ITO: indium tin oxide　　MQW: multi-quantum wells　　SiO_2: silicon dioxide
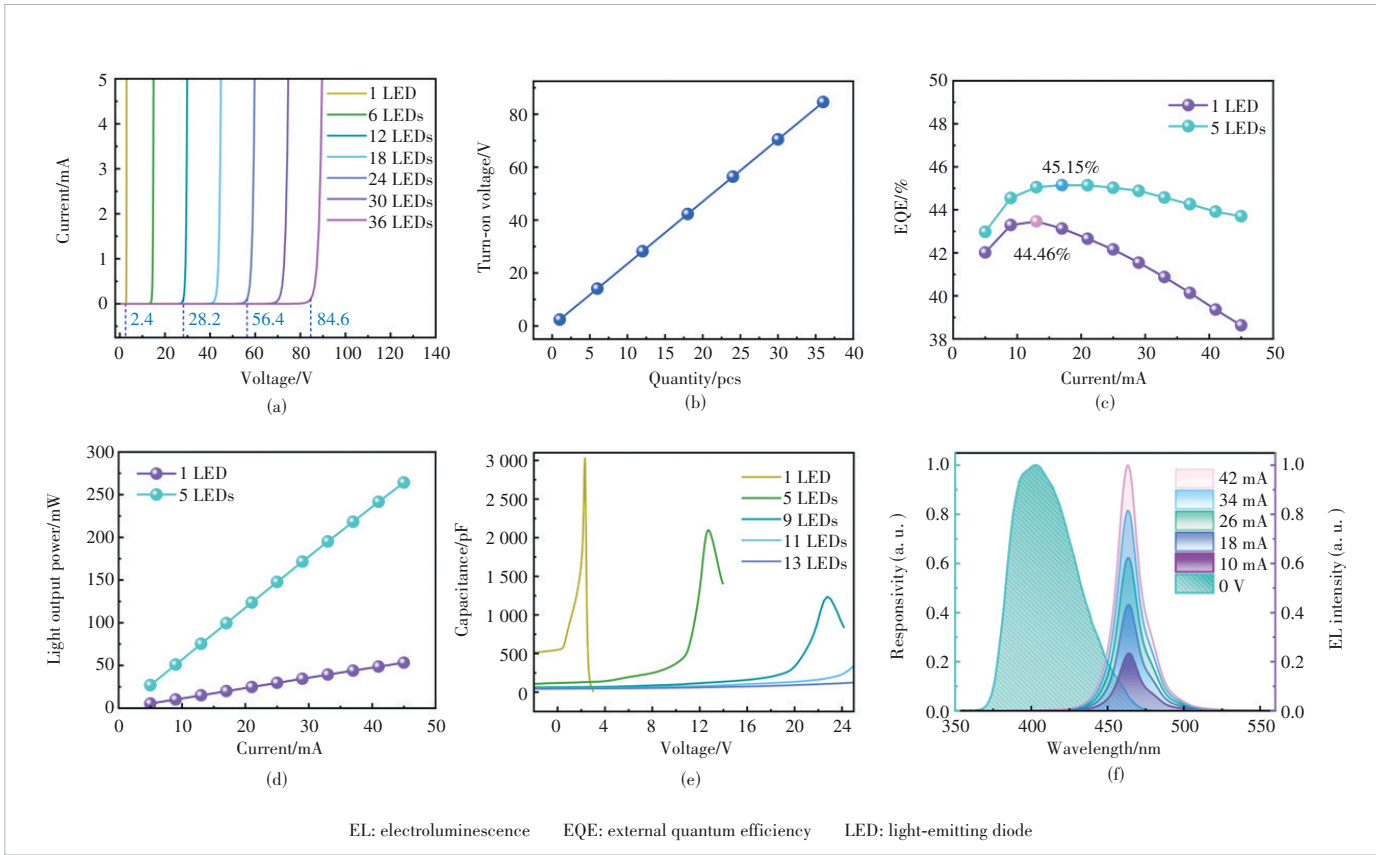
▲Figure 2. Electric and photoelectric characteristics of HVS-LED: (a) IV characteristics of LEDs with different quantities in series; (b) turn-on voltage for different numbers of LEDs in series; (c) EQE for a single LED and five LEDs in series; (d) light output power for a single LED and five LEDs in series; (e) CV curves for different numbers of LEDs in series; (f) the EL spectra and RS of a single LED

(EL) spectra under different injection currents from 10 mA to 42 mA, with peak emission wavelengths of 464 nm. The partial overlap of RS and EL spectra indicates that the light emitted by the HVS-LED can be detected by the identical structure diode employed as a PD.

4 Communication Performance

4.1 GaN MQW Diode Array as a Light Transmitter

Fig. 3a shows a test platform to verify the HVS-LED's ability for communication. A GaN-based HVS-LED is employed as the light transmitter and an avalanche photodiodes (APD) module from Hamamatsu, Japan, with a 4 kHz to 100 MHz bandwidth, is used as the PD. The frequency responses of the HVS-LED are measured by a vector network analyzer (Keysight ENA Network Analyzer E5080A that operates from 9 kHz to 4.5 GHz) configured in a dual-channel setup. One channel is connected to the HVS-LED via a voltage bias module, while the other is directly connected to APD. By utilizing a semiconductor device analyzer (Agilent Technologies B1500A), a DC bias is applied to the HVS-LED, which is then superimposed with a low-power test signal from the vector network analyzer, resulting in their conversion into an optical signal. The optical

signal is subsequently captured by the APD, converted into an electrical signal, and then routed to another channel of the vector network analyzer for visualization.

Fig. 3b depicts the variation in frequency responses of five series-connected LEDs when the injection current increases from 1 mA to 20 mA. The dynamic resistance of the HVS-LED decreases as the bias current increases. This results in more AC signal power being loaded onto the source impedance compared with the load impedance, manifesting as a relative power reduction at higher currents. Furthermore, the 3 dB bandwidth of the device exhibits an increase with the rising injection current, as illustrated in Fig. 3c. This phenomenon can be attributed to the fact that the dynamic resistance of the device decreases due to alterations in the static operating point as the injection current increases, which leads to the expansion of the 3 dB bandwidth.

To determine the relationship between 3 dB bandwidth and LED quantity in series, the injection current on the device is fixed at 5 mA, and the frequency response curves for different numbers of LEDs in series are measured. To directly investigate the impact of LED quantity in series on the device bandwidth, the frequency response of LEDs with different numbers is normalized as shown in Fig. 3d. The 3 dB bandwidth versus

APD: avalanche photodiodes   DC: direct current   LED: light-emitting diode
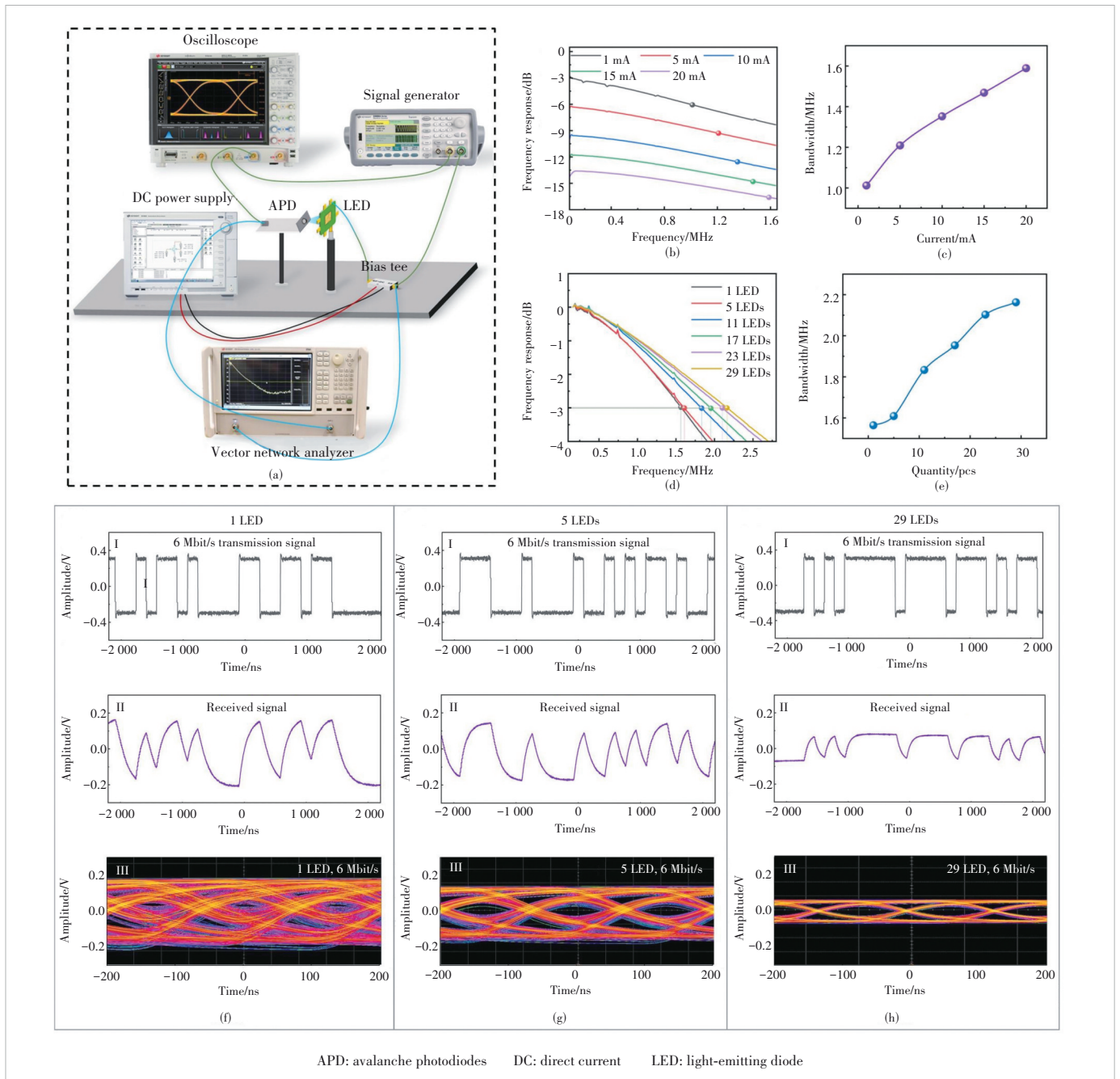
▲Figure 3. Communication performance of HVS-LED: (a) the test platform for verifying HVS-LED's ability for communication; (b) 3 dB bandwidth of the device under different currents when five LEDs are connected in series; (c) 3 dB bandwidth versus injection current; (d) frequency response curves for different numbers of LEDs in series at 5 mA after normalization; (e) 3 dB bandwidth versus LED quantity in series; (f – h) waveform I shows transmission signal curves, waveform Ⅱ received signal curves, and picture Ⅲ eye diagram with a PRBS wave at 6 Mbit/s applied to the device when (f) one LED, (g) five LEDs, and (h) 29 LEDs are connected in series

LED quantity in series is derived from Fig. 3e. The 3 dB bandwidth of the device exhibits an increase with a rising number of LEDs. Theoretically, the bandwidth is inversely proportional to the product of resistance and capacitance. The resistance consists of the source resistance and the LED series resistance. When the LED quantity in series is small, the fixed source resistance plays a dominant role in the total resistance, and the bandwidth increases with the LED quantity due to the decline of capacitance. However, as the LED quantity in series increases to a certain point, the LED series resistance becomes dominant, which is proportional to the quantity and counteracts the capacitance decline. Therefore, the curve trend in Fig. 3e becomes saturated under a large series quantity.

An oscilloscope (Keysight DSOS604A) is utilized to mea-

sure and analyze the received signal. GaN-based HVS-LED is employed as the light transmitter. A functional signal generator (Keysight 33600A Series, Trueform) is configured in a dual-channel setup with one channel connected to the HVS-LED via a voltage bias module, and the other channel connected to the oscilloscope, transmitting a pseudo-random binary sequence (PRBS) signal at 6 Mbit/s. A constant DC bias of 5 mA is applied to the HVS-LED using a semiconductor device analyzer (Agilent Technologies B1500A) to provide high voltage and ensure stable operation. Subsequently, the optical signal of the HVS-LED is captured by an APD, converted into an electrical signal, and then routed to another channel of the oscilloscope for visualization.

Figs. 3f, 3g, and 3h illustrate the corresponding transceiver signals and eye diagrams of a single LED, five LEDs, and 29 LEDs, respectively. Waveform I is the transmitted signal obtained by the oscilloscope directly connected to the signal generator, waveform II is the received signal detected through the optical communication link, and picture III is the corresponding eye diagram of the received signal. It can be observed that the amplitude of the received signal decreases as the number of LEDs increases. The reasons are as follows. The light field emitted by the device expands as the number of LEDs connected in series increases. Since the area of light detected by the APD remains constant, the ratio of detected light intensity to the total light field decreases. Concurrently, while the total AC signal supplied to the device remains unchanged, connecting additional LEDs in series will reduce the AC voltage applied across each LED. These factors collectively contribute to a decrease in the amplitude of the received signal. Furthermore, as the number of series-connected elements increases, the eye diagram of the 6 Mbit/s signal waveform changes from a blurred ribbon line to a distinct and slender trace. This transition is accompanied by a reduction in jitter and noise, as well as an enhancement in the mitigation of inter-symbol interference. This observation indicates the superior communication capabilities of HVS-LED compared to a single GaN MQW diode.

4.2 GaN MQW Diode Array as a PD

The test system to verify the HVS-PD's communication performance is displayed in Fig. 4a. An ultraviolet LED with a 3 dB bandwidth at about 2.55 MHz is employed as a light transmitter and the HVS-PD is utilized as a PD. The peak emission wavelength of the ultraviolet LED is 386 nm, and the electroluminescence spectrum of the ultraviolet LED is completely covered by the response spectrum of the HVS-PD, which means that the ultraviolet LED can be efficiently detected by the HVS-PD. The frequency responses of the HVS-PD are measured by a vector network analyzer (Keysight ENA Network Analyzer E5080A that operates from 9 kHz to 4.5 GHz) configured in a dual-channel setup. One channel is connected to the ultraviolet LED via a voltage bias module,

while the other is directly connected with the HVS-PD. A constant DC bias of 5 mA is applied to the ultraviolet LED. The DC bias signal and the low-power test signal from the vector network analyzer are superimposed on the ultraviolet LED and converted into an optical signal. The optical signal is subsequently captured by the HVS-PD, converted into an electrical signal, and then routed to the channel of the vector network analyzer.

To directly investigate the impact of PD quantity in series on device bandwidth, the frequency responses varying with different numbers of PDs are normalized as shown in Fig. 4b. The 3 dB bandwidth value of each group is marked. The relationship curve between the 3 dB bandwidth and the quantity of PDs in series is obtained in Fig. 4c. It can be found that the 3 dB bandwidth of the device increases with an increasing number of low-power PDs in series. This phenomenon can be attributed to the decrease in capacitance due to the increasing number of PDs connected in series. Furthermore, since the HVS-PD is connected to a high-impedance measurement device, the impact of reduced capacitance outweighs the influence of increased resistance.

An oscilloscope (Keysight DSOS604A) is used to further validate the received signal quality. An ultraviolet LED serves as the light source while the GaN MQW diode array functions as the HVS-PD. The functional signal generator (Keysight 33600A Series, Trueform) is in a dual-channel mode. One channel of the functional signal generator is dedicated to driving the ultraviolet LED, ensuring stable optical signal generation. The other channel transmits a PRBS signal at a bit rate of 1 Mbit/s directly to the oscilloscope for reference and synchronization. The HVS-PD receives and converts the optical signal from the ultraviolet LED into an electrical signal. The electrical signal is amplified to enhance its clarity and signal-to-noise ratio, and then routed to the second channel of the oscilloscope for detailed visualization and analysis of the received signal quality.

The eye diagrams of the communication signals obtained by five PDs and 29 PDs in series are illustrated in Figs. 4d and 4e, respectively. Waveform I is the transmitted signal obtained by the oscilloscope directly connected to the signal generator, waveform II is the received signal detected through the optical communication link, and picture III is the corresponding eye diagram of the received signal. It can be observed that the amplitude of the received signal exhibits an upward trend as the number of PDs increases. Moreover, when operating with five PDs to capture a communication bit rate of 1 Mbit/s, the eye diagram exhibits noticeable noise and jitter. By connecting 29 PDs in series, the reliability of the transmission is enhanced, as evidenced by an increase in the relative amplitude of the eye-opening within the eye diagram. Furthermore, the enlargement of the eye width is indicative of a decrease in jitter, which enhances signal stability and transmission quality. The experimental findings validate improved communication performance of HVS-PD.
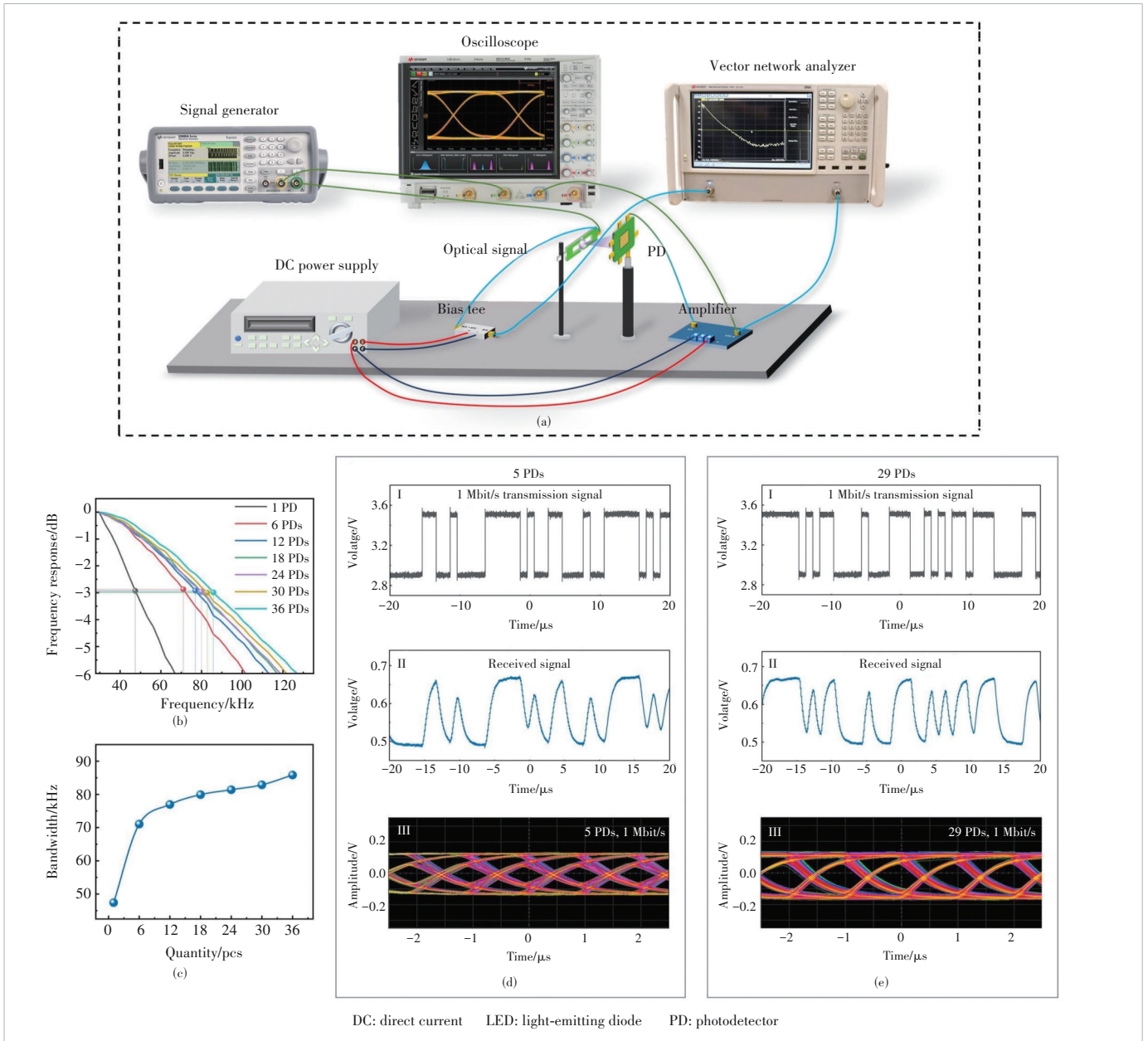
▲Figure 4. Communication performance of HVS-PD: (a) the communication test system; (b) frequency response curves for different numbers of PDs in series with the ultraviolet LED under an injection current of 5 mA; (c) 3 dB bandwidth versus PD quantity in series after normalization; (d – e) waveform Ⅰ shows transmission signal curves, waveform Ⅱ received signal curves, and picture Ⅲ eye diagrams with a PRBS wave at 1 Mbit/s applied to the device when (d) five PDs or (e) 29 PDs are connected in series

5 Conclusions

In this paper, an HVS-LED/PD based on a GaN-integrated photoelectronic chip is designed, and the communication performance of the device is characterized. Experimental results show that the series configuration of GaN MQW diodes significantly enhances output optical power while effectively addressing current spreading issues that may compromise device efficiency. Moreover, as more GaN MQW diodes are connected in series, the 3 dB bandwidth broadens, resulting in a clearer eye diagram. This diagram demonstrates significant

stability and reduced jitter, thereby reflecting an enhancement in communication quality. Moreover, it is expected that the HVS-LED/PD will facilitate potential applications in advanced VLC systems.

References

[1] TAKI T, STRASSBURG M. Review—visible LEDs: more than efficient light [J]. ECS journal of solid state science and technology, 2019, 9(1): 015017. DOI: 10.1149/2.0402001jss

[2] SHEN H B, CAO W R, SHEWMON N T, et al. High-efficiency, low turn-

on voltage blue-violet quantum-dot-based light-emitting diodes [J]. Nano letters, 2015, 15(2): 1211 – 1216. DOI: 10.1021/nl504328f

[3] CHANG Y H, HSU T C, LIOU F J, et al. High-bandwidth InGaN/GaN semipolar micro-LED acting as a fast photodetector for visible light communications [J]. Optics express, 2021, 29(23): 37245 – 37252. DOI: 10.1364/OE.439990

[4] TSAO J Y, CRAWFORD M H, COLTRIN M E, et al. Toward smart and ultra-efficient solid-state lighting [J]. Advanced optical materials, 2014, 2 (9): 809 – 836. DOI: 10.1002/adom.201400131

[5] KRAMES M R, SHCHEKIN O B, MUELLER-MACH R, et al. Status and future of high-power light-emitting diodes for solid-state lighting [J]. Journal of display technology, 2007, 3(2): 160 – 175. DOI: 10.1109/JDT.2007.895339

[6] MERAJ M, RAHMAN S, IQBAL A, et al. High brightness and high voltage dimmable LED driver for advanced lighting system [J]. IEEE access, 2019, 7: 95643 – 95652. DOI: 10.1109/ACCESS.2019.2928859

[7] HUANG Y, GUO Z Y, WANG X J, et al. GaN-based high-response frequency and high-optical power matrix micro-LED for visible light communication [J]. IEEE electron device letters, 2020, 41(10): 1536 – 1539. DOI: 10.1109/LED.2020.3021282

[8] KOMINE T, NAKAGAWA M. Integrated system of white LED visible-light communication and power-line communication [C]//Proc. 13th IEEE International Symposium on Personal, Indoor and Mobile Radio Communications. IEEE, 2002: 1762 – 1766. DOI: 10.1109/PIMRC.2002.1045482

[9] ARVANITAKIS G N, BIAN R, MCKENDRY J J D, et al. Gb/s underwater wireless optical communications using series-connected GaN micro-LED arrays [J]. IEEE photonics journal, 2020, 12(2): 7901210. DOI: 10.1109/JPHOT.2019.2959656

[10] CHU J T, HUANG H W, KAO C C, et al. Fabrication of large-area GaN-based light-emitting diodes on Cu substrate [J]. Japanese journal of applied physics, 2005, 44(4S): 2509. DOI: 10.1143/jjap.44.2509

[11] ZHENG R S, TAGUCHI T. Optical design of large-area GaN-based LEDs [C]//Proc. Light-Emitting Diodes: Research, Manufacturing, and Applications VII. SPIE, 2003: 105 – 112. DOI: 10.1117/12.476554

[12] AVRUTIN V, HAFIZ S A, ZHANG F, et al. Saga of efficiency degradation at high injection in InGaN light emitting diodes [J]. Turkish journal of physics, 2014, 38: 269 – 313. DOI: 10.3906/fiz-1407-23

[13] ZHAN T, ZHANG Y, MA J, et al. Characteristics of GaN-based high-voltage LEDs compared to traditional high power LEDs [J]. IEEE photonics technology letters, 2013, 25(9): 844 – 847. DOI: 10.1109/LPT.2013.2251878

[14] FAN Z Y, LIN J Y, JIANG H X. III-nitride micro-emitter arrays: development and applications [J]. Journal of physics D: applied physics, 2008, 41 (9): 094001. DOI: 10.1088/0022-3727/41/9/094001

[15] ZHAN T, ZHANG Y, LI J, et al. The design and fabrication of a GaN-based monolithic light-emitting diode array [J]. Journal of semiconductors, 2013, 34(9): 094010. DOI: 10.1088/1674-4926/34/9/094010

[16] FAN X, GUO W L, SUN J. Reliability of high-voltage GaN-based light-emitting diodes [J]. IEEE transactions on device and materials reliability, 2019, 19(2): 402 – 408. DOI: 10.1109/TDMR.2019.2917005

[17] ZHANG Y B, XU J W, DING M D, et al. Wafer-level light emitting diode (WL-LED) chip simplified package for very-high power solid-state lighting (SSL) source [J]. IEEE electron device letters, 2016, 37(2): 197 – 200. DOI: 10.1109/LED.2015.2509462

[18] CHEN Z H, ZHANG Q, WANG K, et al. Reliability test and failure analysis of high power LED packages [J]. Journal of semiconductors, 2011, 32(1): 014007. DOI: 10.1088/1674-4926/32/1/014007

[19] WANG C H, LIN D W, LEE C Y, et al. Efficiency and droop improvement in GaN-based high-voltage light-emitting diodes [J]. IEEE electron device letters, 2011, 32(8): 1098 – 1100. DOI: 10.1109/LED.2011.2153176

[20] TIEN C H, CHEN K Y, HSU C P, et al. Enhanced light output power of thin film GaN-based high voltage light-emitting diodes [J]. Optics express, 2014, 22(S6): A1462. DOI: 10.1364/oe.22.0a1462

[21] ZHOU S J, ZHENG C J, LV J J, et al. Effect of profile and size of isolation trench on the optical and electrical performance of GaN-based high-voltage LEDs [J]. Applied surface science, 2016, 366: 299 – 303. DOI: 10.1016/j.apsusc.2016.01.068

[22] ZHOU S J, YUAN S, LIU Y C, et al. Highly efficient and reliable high power LEDs with patterned sapphire substrate and strip-shaped distributed current blocking layer [J]. Applied surface science, 2015, 355: 1013 – 1019. DOI: 10.1016/j.apsusc.2015.07.194

[23] KORNIENKO V, KRISTENSSON E, EHN A, et al. Beyond MHz image recordings using LEDs and the FRAME concept [J]. Scientific reports, 2020, 10(1): 16650. DOI: 10.1038/s41598-020-73738-1

[24] O'HAGAN W J, MCKENNA M, SHERRINGTON D C, et al. MHz LED source for nanosecond fluorescence sensing [J]. Measurement science and technology, 2002, 13(1): 84 – 91. DOI: 10.1088/0957-0233/13/1/311

[25] LI X, HAN M Y, CHEN M P, et al. Integrated sensing and communication chip based on III-nitride for motion detection [J]. ACS omega, 2023, 8(16): 14656 – 14661. DOI: 10.1021/acsomega.3c00521

[26] WANG Y J, GAO Y, WANG L L, et al. Underwater blue light communication using vertical-structure GaN light emitting diode [J]. Journal of electronics and information technology, 2022, 44(8): 2703 – 2709. DOI: 10.11999/JEIT220328

[27] JAMES SINGH K, HUANG Y M, AHMED T, et al. Micro-LED as a promising candidate for high-speed visible light communication [J]. Applied sciences, 2020, 10(20): 7384. DOI: 10.3390/app10207384

Biographies

LU Meixin is an undergraduate at the School of Communication and Information Engineering, Nanjing University of Posts and Telecommunications, China. Her research focuses on sensors, GaN-based optoelectronic devices, and visible light communications systems.

JIANG Zitong is an undergraduate at the School of Communication and Information Engineering, Nanjing University of Posts and Telecommunications, China. Her research focuses on quantum sensing technology, strong magnetic field measurement, and visible light communications systems.

FANG Li received his BS degree in electronic information engineering from Qingdao University of Technology, China in 2022. He is currently pursuing an MS degree in electronic information with the Nanjing University of Posts and Telecommunications, China. His current research interests include GaN-based optoelectronic devices, optoelectronic integrated circuit (OEIC), thermoelectric/photoelectric energy harvesters, and RF MEMS devices.

YAN Yiqun received her BS degree in communication engineering from Qingdao University of Technology, China in 2023. She is currently pursuing an MS degree in electronic information with the Nanjing University of Posts and Telecommunications, China. Her current research interests include GaN-based optoelectronic devices, acoustic sensors, and photoelectric energy harvesters.

YAN Jiabin (jbyan@njupt.edu.cn) received his BS degree in microelectronics from Shanghai University, China and PhD degree in microelectronics and solid state electronics from Southeast University, China in 2013 and 2018, respectively. He is currently an associate professor with the Peter Grünberg Research Center, Nanjing University of Posts and Telecommunications, China. The discipline of his research focuses on GaN-based optoelectronic devices, optoelectronic integrated circuit (OEIC), thermoelectric/photoelectric energy harvesters, and RF MEMS devices.